

Response to Review 1

(Review comments in *Italic*, response in upright Roman)

The manuscript describes a dataset measured by the Lake Taihu Eddy Flux Network which consists of seven eddy covariance (EC) flux stations over Lake Taihu and one EC flux tower over the land as a reference. Although EC flux measurements over inland waters have increased worldwide, such a flux network over a single lake is rare. Besides the uniqueness of the dataset stated in the manuscript, it could provide a valuable perspective in terms of spatial variability in fluxes and associated controlling factors. The dataset should benefit to broader communities in micrometeorology, hydrology, remote sensing, water resource managements, and modeling to name a few. The descriptions of the sites, instruments, and methods are clear and adequate. The dataset is of high quality as also reflected by their published research articles (I read most of them in the past). The manuscript is well written and structured. I would recommend its publication.

Thank you.

Here are a few minor comments:

I understand water levels vary, but would it be good to provide the lake bathymetry also with the tower locations to give users a better understanding of the lake?

Do you have water level measurements or provide information that helps users to find how water levels vary?

The daily water level is monitored by the TAIHU BASIN AUTHORITY at five locations around the lake (<http://www.tba.gov.cn/slbthlyglj/sj/sj.html>), as shown in Figure R1 below. Using this time series, we have constructed the water depth for our eddy covariance sites (Figure R2, added to the revision as Figure 2).

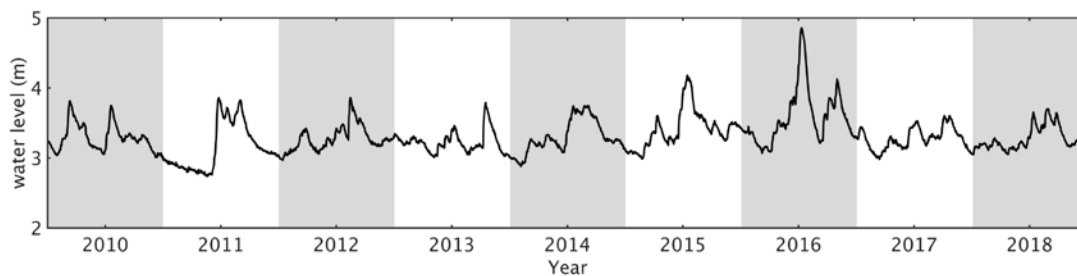


Figure R1. Daily water level (above local sea level) in Lake Taihu

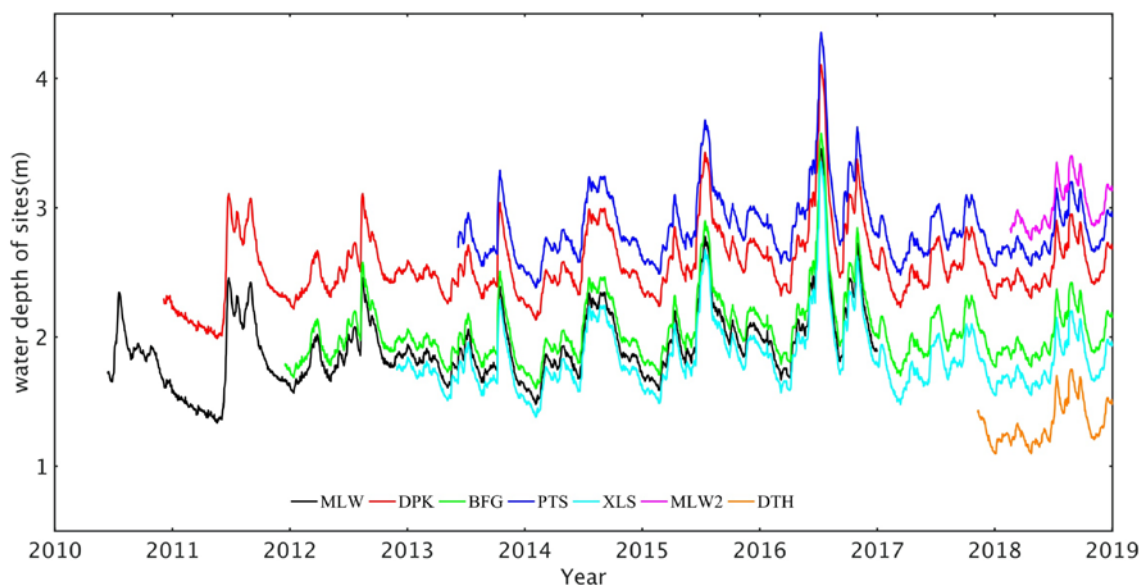


Figure R2 Water depth at the eddy covariance sites

We have added the following text to the revision:

“The lake water level is monitored daily by the Taihu Basin Authority (<http://www.tba.gov.cn/>) at five locations around the lake. Using the water-level time series, we have constructed the water depth for our eddy covariance sites (Figure 2).”

Line 130-131: This may be a little bit misleading since the heights for the lake sites vary from 3.5 to 9.4 m and the EC height for the land site is 20 m.

Thank you. This sentence has been changed to “The EC instrument is at a height of 3.5 to 9.4 m above the water surface at the lake sites and at a height of 20 m above the ground at the land site.”

Please explain how you keep these sensors in such fixed depths.

We have added the following explanation:

“The top four sensors were tied to a nylon rope hanging from a buoy to ensure that they were at the designed depths regardless of water level fluctuations.”

Response to Review 2

(Review comments in *Italic*, response in upright Roman)

In this manuscript, the authors describe a significant database of eddy-covariance and micro-meteorological measurements over a large lake in China. The data is collected by an eddy flux network consisting of seven lake and one land eddy-covariance towers. Data is collected from 2010 to 2018. The data presented will be valuable for researchers in various disciplines like air-water interactions, climate and weather modeling, and water management. The manuscript is generally well written, and the authors presented the necessary information. I have several comments that the authors should consider upon revision of the manuscript. The comments are provided on the attached PDF file.

Thank you for your careful review of our manuscript.

Line 23: replace "upland" with "land"

Done.

Line 28: half-hourly intervals: I guess these are half-hourly averages.

We have changed the sentence to “Data variables are saved as half-hourly averages...”

Line 47 deployed: replace "deployed" with "employed"

Done

Line 52 upland: replace "upland" with "land"

Done

Line 73 deployed: replace "deployed" with "employed"

Done

Line 126 EC system for long-term monitoring: For the lake stations, you should explain briefly how did you install the stations. Did you install the sensors on stationary or floating platforms? Floating platform may be susceptible to oscillations due to water waves, which may affect sensors' readings.

In response, we have added the following text for clarity

“Measurements at the lake sites were made on fixed platforms. Readers are referred to Lee et al. (2014) and Xiao et al. (2017) for photographs of the platform and the instruments.”

Line 129 infrared analyzer: add "gas" between "infrared" and "analyzer"

Corrected

Line 131: instrument: replace "instrument" with "system"

Corrected

Line 138 the DS land site: Did you measure soil heat flux at the land site?

We did monitor soil heat flux at the 5-cm depth at DS. The data and data flag are added as columns 33 and 34. The dataset on Harvard Dataverse and on our website have been updated. Thank you.

Line 142-147 If methane flux is not included in this paper, there is no need to provide all these details. I suggest removing this paragraph.

Removed.

Line 149 EC covariance: EC is eddy covariance so the word "covariance" appears twice.

Corrected

Q12: *Line 150: natural coordinate system: Please provide a more specific explanation of this system, and its consequence for potential users of the data.*

We have added the following explanation:

“In this coordinate system, the longitudinal coordinate axis is aligned with the 30-min mean velocity vector so that the 30-min mean lateral and vertical velocity components are zero and the magnitude of the mean velocity is equal to the mean longitudinal component, and the covariance between the lateral and the vertical velocity components is zero.”

Line 159: proportions of data with quality flag 0: What is the meaning of this quality flag? Please give some explanation.

We have expanded the sentence to

“... where the percentage values represent the proportions of data with quality flag 0, which indicates high-quality original measurement (Table 3).”

Q14: *Line 179: Data Quality Flags: The description of data quality flags is confusing since you do not refer to the common quality flags used in the eddy covariance methodology. The commonly used flags are related to the validity of steady state and turbulence development conditions. Please revise the text to better clarify this issue.*

For clarification, we have modified the text to

“Each data variable is assigned a quality flag to distinguish original measurements and gap-filled values and gap-filling methods (Table 3). The data flags employed here should not be confused with quality flags commonly assigned to the EC methodology in the literature. Specifically, Flag 0 indicates high-quality original data. Other flag values indicate gap-filled data or missing values.”

Q15: *Line 201-202 “... Compared to the original data, the gap-filled data do not capture the full diurnal variations.” Explain why?*

An explanation is added as

“Compared to the original data, the gap-filled data do not capture the full diurnal variations because the 5-cm soil temperature has smaller diurnal amplitudes than the soil surface temperature, but the daily-mean upward longwave radiation flux seems reasonable.”

Q16: *Line 207 the bulk transfer relationship: I guess this relationship is extracted from another site where data is not missing? Please explain.*

This relationship is established for each site using data collected during periods when data on both the flux and the state variables were available. We have modified the text to improve clarity:

“The transfer coefficient C_H is determined from the observed H and the state variables (U , T_a and T_s) outside the gap periods. The missing data on H is then filled with the above relationship using the tuned C_H the observed U , T_a and T_s .”

Line 240: remove "the"
Corrected.

Line 240 (Table 4): replace "Table 4" with "Table 1"
Corrected.

Line 245: remove "and"
Corrected.

Line 247-248 "2012, 1, 12, 00": I think "month" or "day" are missing.
We have changed it to “2012, 1, 1, 12, 00”

Line 265: Which station?
We have changed to: “the four WMO stations.”

Line 278: add "is" before "net"
Corrected.

Line 313: replace "2010" with "2018"
Corrected.

Q24: *Line 339: Percent of data coverage: Explain more specifically what are these percentages.*

The table caption has been modified as: “**Table 2.** Percent of data coverage. The percentage represents the proportion of high-quality original measurement.”

Line 350: add "half-hourly" between "an" and "observation"
Corrected.

Line 359: In the map, I recommend adding names of some major cities of China for easier orientation of the lake location in China.
Done.

Line 359: Indicate which sites are on the lake and which is on the land.
Done.

368 Figure 2: This figure is not mentioned in the text.
This figure is now cited in the main text.

Line 387: replace "bar" with "bars"
Corrected.

Line 387: replace "represents" with "represent"
Corrected.

Line 387 (line): If the values are annual means, the lines connecting the points have no meaning. Please revise.

We include lines to help better visualize inter-annual variability.

Line 393 latent heat flux: This is not the observed LE as indicated on the Y-axis label, but LE adjusted for energy balance closure. This should be indicated.

This is a very good point. We have changed the Y-axis label to "Monthly LE"

1 **A dataset of microclimate and radiation and energy fluxes from the Lake Taihu Eddy**

2 **Flux Network**

3 Zheng Zhang^{a,b}, Mi Zhang^{a,b,d}, Chang Cao^{a,b}, Wei Wang^{a,b}, Wei Xiao^{a,b,d}, Chengyu Xie^{a,b},
4 Haoran Chu^{a,b}, Jiao Wang^{a,b}, Jiayu Zhao^{a,b}, Lei Jia^{a,b}, Qiang Liu^{a,b}, Wenjing Huang^{a,b},
5 Wenqing Zhang^{a,b}, Yang Lu^{a,b}, Yanhong Xie^{a,b}, Yi Wang^{a,b}, Yini Pu^{a,b}, Yongbo Hu^{a,b}, Zheng
6 Chen^{a,b}, Zhihao Qin^{a,b}, Xuhui Lee^{c*}

7
8 a Yale-NUIST Center on Atmospheric Environment, International Joint Laboratory on
9 Climate and Environment Change (ILCEC), Nanjing University of Information Science and
10 Technology, Nanjing, Jiangsu Province, China

11
12 b Key Laboratory of Meteorological Disaster, Ministry of Education and Collaborative
13 Innovation Center on Forecast and Evaluation of Meteorological Disasters, Nanjing
14 University of Information Science and Technology, Nanjing, Jiangsu Province, China

15
16 c School of Forestry and Environmental Studies, Yale University, New Haven, CT, USA

17
18 d NUIST-Wuxi Research Institute, Wuxi, Jiangsu Province, China

19 * Corresponding author: xuhui.lee@yale.edu

20

21 **Abstract**

22 Eddy covariance data are widely used for the investigation of surface-air interactions.

23 Although ~~numerous~~^{several} datasets exist in public depositories for ~~up~~land ecosystems, few
24 research groups have released eddy covariance data collected over lakes. In this paper, we
25 describe a dataset from the Lake Taihu Eddy Flux Network, a network consisting of seven
26 lake sites and one land site. Lake Taihu is the third largest freshwater lake (area 2,400 km²) in
27 China, under the influence of subtropical climate. The dataset spans the period from June
28 2010 to December 2018. Data variables are ~~recorded as~~^{saved} half-hourly ~~average~~^{intervals}
29 and include micrometeorology (air temperature, humidity, wind speed, wind direction,
30 rainfall, and water/soil temperature profile), the four components of surface radiation balance,
31 friction velocity, and sensible and latent heat fluxes. Except for rainfall and wind direction,
32 all other variables are gap-filled, with each datapoint marked by a quality flag. Several areas
33 of research can potentially benefit from the publication of this dataset, including evaluation
34 of mesoscale weather forecast models, development of lake-air flux parameterizations,
35 investigation of climatic controls on lake evaporation, validation of remote sensing surface
36 data products, and global synthesis on lake-air interactions. The dataset is publicly available
37 at <https://yncenter.sites.yale.edu/data-access> and from Harvard Dataverse
38 [https://dataverse.harvard.edu/dataset.xhtml?persistentId=doi:10.7910/DVN/HEWCWM&version=DRAFT&fac](https://dataverse.harvard.edu/dataset.xhtml?persistentId=doi:10.7910/DVN/HEWCWM&version=DRAFT&faces-redirect=true)
39 [es-redirect=true https://doi.org/10.7910/DVN/HEWCWM](https://doi.org/10.7910/DVN/HEWCWM) (Zhang et al., 2020)

40

41

42 **1. Introduction**

43 Inland lakes and reservoirs are a vital freshwater resource for the society. Globally, there are
44 more than 27 million water bodies with size greater than 0.01 km², occupying a total of 3.5%
45 of the Earth's land surface area (Downing et al., 2006; Verpoorter et al., 2014). Accurate
46 observation of the lake microclimate and lake-air interactions will help to better manage this
47 water resource and to better predict how it may be affected by environmental changes.

48 Towards that end, an increasing number of studies have employed the eddy covariance (EC)
49 methodology to monitor physical state (temperature, wind, humidity) and process variables
50 (momentum flux, and radiation and energy fluxes) in the lake environment (Vesala et al.,
51 2006; Blanken et al., 2011; Nordbo et al., 2011; Wang et al., 2014; Li et al., 2015; Yusup and
52 Liu, 2016; Du et al., 2018; Hamdani et al., 2018; Xiao et al., 2018; Wang et al., 2019). Unlike
53 EC studies in upland ecosystems, however, data from these lake studies are rarely published
54 as data papers or are archived in public data depositories accessible by the broader scientific
55 community. For example, of the nearly 500 sites that have contributed EC and
56 micrometeorological data to AmeriFlux, a public data depository
57 (<https://ameriflux.lbl.gov/data/data-availability/>), none is a lake site. Although a few
58 scientific groups have provided data supplements to their scientific papers on lake-air fluxes
59 (e. g., Charusombat et al., 2018; Franz et al., 2018; Zhao and Liu, 2018), we are not aware of
60 a data paper devoted to systematic description and archival of EC lake observations.

61
62 In this paper, we describe the dataset from the Lake Taihu Eddy Flux Network (Lee et al.,
63 2014). Established in 2010, the network currently consists of six active lake sites, one

64 inactive lake site, and one active land site. Lake Taihu is the third largest freshwater lake
65 (area 2,400 km²) in China. Data variables are recorded at half-hourly intervals and the
66 measurement has continued for over eight years. Several areas of research can potentially
67 benefit from the publication of this dataset, including evaluation of mesoscale weather
68 forecast models, development of lake-air flux parameterizations, investigation of climatic
69 controls on lake evaporation, validation of remote sensing surface data products, and global
70 synthesis on lake-air interactions.

71
72 This paper is organized as follows. Section 2 is a brief overview of the sites and the
73 instruments used by the network. This is followed, in Section 3, with a description of data
74 quality measures ~~em~~deployed during the field monitoring. Section 4 provides the essential
75 information about the dataset, including data variables, gap-filling methods, and data quality
76 flags. Results of post-field evaluation of the data quality are given in Section 5.

77
78 Users of this dataset may be interested in the relevant papers published by our group. Lee et
79 al. (2014) gave an overview of the Lake Taihu Eddy Flux Network. Using the data collected
80 at a subset of the sites and during the early phase of the network, Wang et al. (2014)
81 investigated the spatial variability of energy and momentum fluxes across the lake. Xiao et al.
82 (2013) improved the bulk parameterizations of heat, water and momentum fluxes for shallow
83 lakes. Deng et al. (2013) and Hu et al. (2017) modified the CLM lake simulator (Subin et al.,
84 2012) to improve its prediction of the lake evaporation. Wang et al. (2017) and Zhang et al.
85 (2019b) evaluated the performance of two mesoscale models of the lake-land breeze. More

86 recently, Xiao et al. (2020, manuscript in review) investigated drivers of the interannual
87 variability of the lake evaporation observed at one of the lake sites (BFG). The value of the
88 dataset is enhanced by these peer-reviewed publications because they have helped us to
89 continuously improve our measurement and data processing protocols. For example, we have
90 used the locally-calibrated bulk parameterizations of Xiao et al. (2013) to gap-fill the flux
91 variables.

92

93 **2. Sites and Instrumentation**

94 **2.1 Sites and data periods**

95 Table 1 shows the basic site information and Figure 1 is a map that gives the relative position
96 of Lake Taihu in China and locations of the EC measurement sites. Also shown in Figure 1
97 are WMO baseline weather stations around the lake, whose data can be obtained from
98 National Meteorological Information Center in China (<http://data.cma.cn/site/index.html>).
99 The lake, located between the latitudinal range of 30°5'40" N to 31°32'58" N and
100 longitudinal range of 119°52'32" E to 120°36'10" E, has a total area of 2400 km² and an
101 average depth of 1.9 m. The climate is subtropical monsoon, with an annual mean
102 temperature of 16.2°C and annual total precipitation of 1122 mm. The lake is ice-free
103 throughout the year.

104

105 The EC network consists of seven lake sites and one land site. The lake sites (Meiliangwan
106 (MLW), Dapukou (DPK), Bifenggang (BFG), Xiaoleishan (XLS), Pingtaishan (PTS),
107 Dongtaihu (DTH), Meiliangwan2 (MLW2)) are distributed according to biological

108 characteristics and across eutrophication gradients of the lake. The MLW site, located in
109 Meiliangwan Bay near the north shore of Lake Taihu, was the first site in operation; the
110 measurement began in June 2010 and was replaced by MLW2 in 2018, at 10 km southwest of
111 MLW. Both MLW and MLW2 sites are located in the lake eutrophic zone. BFG is located in
112 the east part of Lake Taihu in relatively clean water inhabited by submerged vegetation with
113 a growth season from April to November. DTH is located in the shallow water (mean depth
114 of 1.3 m) in the southeast part of the lake. After more than 20 years of crab aquaculture, this
115 zone was returned to unmanaged state in December 2018 in order to improve water quality.
116 The observation at DTH enables the examination of lake-air exchange processes in the
117 transition from human management to a natural state. PTS is situated in the middle of Lake
118 Taihu where occasional algal blooms occur and no aquatic vegetation is present. DPK is
119 located near the west shore, in a relatively deep (depth 2.5 m) super eutrophic zone due to
120 heavy influence of agricultural and urban runoffs. XLS is located in the relatively clean and
121 vegetation-free zone in the southeast. Finally, DS is a land site surrounded by rice agriculture,
122 serving as a land reference for the lake sites. The MLW site is situated at a distance of 200 m
123 from the north shore of the lake. All the other lake sites in the lake are at a distance of more
124 than 1 km away from the land.

125
126 The lake water level is monitored daily by the Taihu Basin Authority at five locations around
127 the lake (<http://www.tba.gov.cn/>). Using the water-level time series, we have constructed the
128 water depth for our eddy covariance sites (Figure 2).

129

130 **2.2 Instrumentation**

131 Each site is equipped with an EC system for long-term, continuous monitoring of the surface
132 momentum, sensible heat, latent heat and carbon dioxide fluxes. The EC system consists of a
133 sonic anemometer/ thermometer (Model CSAT3A; Campbell Scientific, Logan, UT, USA)
134 and a CO₂/H₂O infrared gas analyzer (Model 7500A, LI-COR, Inc., Lincoln, NE, USA at DS,
135 MLW, MLW2 and DPK; Model EC150, Campbell Scientific at other sites). The EC system
136 is at a height of 3.5 to 9.4 m above the water surface at the lake sites and at a height of 20 m
137 above the ground at the land site.~~The EC instrument is at a height of 3.5 to 20 m above the~~
138 ~~water or the soil surface.~~ Other measurements include air humidity and air temperature
139 (Model HMP45D/HMP155A; Vaisala, Inc, Helsinki, Finland), wind speed and wind
140 direction (Model 03002; R. M. Young Company, Traverse City, MI, USA) and four
141 components of the net radiation (Model CNR4; Kipp & Zonen B. V., Delft, the Netherlands).
142 At the lake sites, water temperature profile was measured with temperature probes (Model
143 109-L; Campbell Scientific) at the water depth of 20, 50, 100, and 150 cm and in the
144 sediment at about 5 cm below bottom of the water column. The top four temperature sensors
145 were tied to a nylon rope hanging from a buoy to ensure that they were at the designed depths
146 regardless of water level fluctuations. At the DS land site, soil temperature profile was
147 measured with the same type of probes at the depths of 5, 10, 20 cm. The MLW and the DS
148 sites are supported by A/C power and other sites are powered by battery packs connected to
149 solar panels.
150 Measurements at the lake sites were made on fixed platforms. Readers are referred to Lee et
151 al. (2014) and Xiao et al. (2017) for photographs of the platform and the instruments.

152
153 ~~The methane flux was measured at MLW, BFG and DTH for selected periods, in addition to~~
154 ~~the standard variables described above, using a flux gradient system (at MLW; Xiao et al.~~
155 ~~2014) and an open path eddy covariance system (at BFG and DTH, Zhang et al., 2019a). The~~
156 ~~carbon dioxide and methane flux data are not included in the current version of the data~~
157 ~~release but will be added at a later time after the data quality has been fully examined and the~~
158 ~~data gaps filled.~~

159
160 All the variables are reported as 30-min averages. The EC ~~covariance~~ data are expressed in
161 the natural coordinate system (Lee et al., 2004). In this coordinate system, the longitudinal
162 coordinate axis is aligned with the 30-min mean velocity vector so that the 30-min mean
163 lateral and vertical velocity components are zero and the magnitude of the mean velocity is
164 equal to the mean longitudinal component, and the covariance between the lateral and the
165 vertical velocity components is zero. Additionally, a small density correction has been
166 applied to the water vapor flux according to Webb et al. (1980).

Formatted: Left

168 **3 Data Quality Control during Field Monitoring**

169 Every site in the Lake Taihu Eddy Flux Network is equipped with a wireless transmission
170 module for real-time monitoring and for data transmission. Time series of all 30-min
171 variables are examined weekly and abnormal behaviors are flagged for site operators. Each
172 site is visited every one to two months to perform instrument repair and maintenance and to
173 download 10 Hz EC data. The data coverage rates are summarized in Table 2, where the

174 percentage values represent the proportions of data with quality flag 0, which indicates
175 high-quality original measurement –(Table 3).

176
177 The four-way net radiometers at MLW and XLS were compared in the field against a
178 laboratory standard of the same type in the summer of 2018 to check their long-term stability.
179 (Figure 3). These two sites were chosen because they have been in operation for more than
180 five years. Additionally, the radiometer at MLW was relocated to MLW2 after MLW had
181 been discontinued. The laboratory standard, which had been calibrated at the manufacturer
182 prior to this performance evaluation, was mounted next to the field instrument for about 10
183 days at each site, covering overcast to clear-sky conditions. The mean bias error was smaller
184 than 1 W m^{-2} for all the radiation components. It was -0.81, -0.81, 0.79 and -0.44 W m^{-2} for
185 the downward shortwave, upward shortwave, downward longwave and upward longwave
186 radiation flux at MLW, respectively. The corresponding values were 0.91, 0.40, 0.69 and
187 0.77 W m^{-2} for XLS. (Comparison experiments are being planned for the other sites.)

188
189 The EC gas analyzers were calibrated every one to two years. The zero-point calibration was
190 carried out with high-purity nitrogen gas, the CO_2 span calibration was made with standard
191 carbon dioxide gases (in the concentration range of 389 to 525 ppm) provided by the National
192 Institute of Meteorology (NIM), China and certified to an accuracy of 1%, and the H_2O span
193 calibration was made with a portable dew-point generator (LI-610; LI-COR, Inc.).

194

195 **4. Gap-filling Methods and Data Quality Flags**

196 We use five-point moving average to screen outliers. If the deviation from the moving
197 average is greater than two standard deviations, the data point is discarded. If a gap length is
198 30 min to 1 h, the gap is filled by linear interpolation. Larger gaps in meteorological variables,
199 radiation components and water temperature are filled with linear regression involving
200 observation of the same variable at another site. This spatial interpolation consists of three
201 steps. First, linear correlation is calculated using the valid data at the target site and at all
202 other sites for the month during which the data gap occurred. Second, the observation at the
203 site with the highest linear correlation is used to establish a linear regression equation. Third,
204 the gap at the target site is filled with the linear regression and the observation at that site.

205

206 Radiation data gaps at the DS land site require special treatment. The radiometer at DS eddy
207 flux site ended in January 2013. Subsequent measurements of the radiation component are
208 provided by a radiometer belonging to the Dongshan WMO weather station at a distance of
209 50 m from the eddy covariance tower (Figure 1). While large gaps in meteorological
210 variables (air temperature, relative humidity, wind speed and air pressure), downward solar
211 radiation and downward longwave radiation are filled with the spatial interpolation method,
212 large gaps in upward shortwave radiation and upward longwave radiation cannot be filled
213 with data from other lake sites even with linear regression. In the case of the upward
214 shortwave radiation, the data gaps were filled using the relationship between downward
215 shortwave radiation and the monthly mean albedo. In the case of upward longwave radiation,
216 the data gaps were filled by a regression equation between the upward longwave radiation
217 and the fourth power of soil temperature at 5-cm depth. Compared to the original data, the

218 gap-filled data do not capture the full diurnal variations because the 5-cm soil temperature
219 has smaller diurnal amplitudes than the soil surface temperature. but the daily-mean upward
220 ~~shortwave and~~ longwave radiation fluxes seem reasonable.

221
222 Large data gaps in the EC variables (sensible heat flux, latent heat flux and friction velocity)
223 are filled with a hybrid method. First, if observations exist for the relevant state variable, the
224 gap is filled with the bulk transfer relationship using a ~~locally-tuned~~ transfer coefficient tuned
225 locally for each site (Xiao et al., 2013). For example, the relationship for filling gaps in the
226 sensible heat flux is

$$H = \rho_a c_p C_H U (T_s - T_a)$$

227
228 where ρ_a is air density, c_p is specific heat of air at constant pressure, C_H is the transfer
229 coefficient for sensible heat, T_a is air temperature and T_s is water surface temperature. The
230 transfer coefficient C_H is determined from the observed H and the state variables (U , T_a and
231 T_s) outside gap periods. The missing data on H is then filled with the above relationship using
232 the tuned C_H the observed U , T_a and T_s . Second, if data for the state variable is missing, the
233 spatial interpolation method is used to fill the gaps in these EC variables.

234
235 The spatial interpolation method described above occasionally causes a sudden jump at the
236 beginning or end of a data gap. To harmonize the data, we apply a 5-point moving averaging
237 to the gap-filled time series. If a data point deviates by 2 times of the standard deviation from
238 the moving average, it is replaced by linear interpolation using the two adjacent data points.

239

Formatted: Font: Italic

Formatted: Font: Italic

Formatted: Font: Italic

Formatted: Font: Italic

240 Each data ~~variablepoint~~ is assigned a quality flag to distinguish original measurements and
241 gap-filled values and gap-filling methods (Table 3). The data flags employed here should not
242 be confused with quality flags commonly assigned to the EC methodology in the literature.
243 Specifically, Flag 0 indicates high-quality original data. Other flag values indicate gap-filled
244 data or missing values. Flag 1 indicates that the data was filled by temporal interpolation.
245 Flag 2 indicates that the data was filled by the spatial interpolation method. Flag 3 for the EC
246 variables indicates that the data was filled by the bulk relationship. We also use Flag 3 to
247 mark the upward shortwave and longwave radiation data filled with the albedo and the
248 surface temperature relationship, respectively, for the DS land site. Missing values occur on
249 some situations, which are marked with Flag 4. Figure 43 is an example showing the
250 gap-filled time series of several variables at BFG along with the flag status.

251
252 Rainfall data has not been quantity-controlled or gap-filled. Because of the episodic nature of
253 rainstorms and high spatial variability of rainfall, it is not appropriate to fill data gaps with
254 the time or spatial interpolation method. The total rain amount is likely biased low because
255 no wind screens are used to protect the rain gages from the influence of wind which is much
256 higher on the lake than on land (Figure 54 below). On several site visits, the drain opening to
257 the tipping bucket was found to be partially blocked by debris. Rain amount at a constant and
258 low rate and excessively long rain duration are evidence of such blockage. The flag status of
259 0 for the rainfall variable simply indicates that the field measurement is available, but it does
260 not guarantee high data quality.

261

262 The data coverage begins from the start time of each site (Table 14) and ~~the~~ ends in
263 December 2018. The time resolution is 30 min. The dataset includes microclimate variables
264 (air pressure, air temperature, relative humidity, wind speed, wind direction and rainfall),
265 radiation fluxes (upward and downward shortwave radiation, upward and downward
266 longwave radiation), water temperature at depth of 0.2 m, 0.5 m, 1.0 m and 1.5 m, and in the
267 5-cm sediment) and eddy fluxes (friction velocity, ~~and~~ sensible heat and latent heat fluxes;
268 Table 4). The time stamp is Beijing time (UTC + 8 h) given by data columns 1 to 5 as year,
269 month, day, hour, and minute, and marks the end of the observation period. For example,
270 time stamp “2012, 1, 1, 12, 00” indicates that the data acquisition period is from 11:30 to
271 12:00 on January 1, 2012.

272
273 Although the data table does not include the radiative surface temperature T_s , the user can
274 easily calculate it from the two longwave radiation fluxes, as

275
$$T_s = \left(\frac{L_{\uparrow} - (1 - \varepsilon)L_{\downarrow}}{\varepsilon\sigma} \right)^{\frac{1}{4}}$$

276 where σ is the Stefan-Boltzmann constant, ε is emissivity, and L_{\uparrow} and L_{\downarrow} are upward and
277 downward longwave radiation flux, respectively. We use a value of 0.97 for lake surface
278 emissivity in this calculation (Deng et al., 2013; Wang et al., 2014).

279

280 5. Data Consistency Evaluation

281 Figure 54 compares the annual mean air temperature, relative humidity, and wind speed at
282 the Taihu eddy flux sites with those at the four WMO weather stations (Wuxi, Liyang,

283 Huzhou and Dongshan) around the lake (Figure 1). The error bars represent the maximum
284 and minimum values among the four WMO stations and the lines represent the mean values
285 of the four station measurements. The annual mean air temperature at DTH is 0.3°C higher
286 than the station mean. At other sites, air temperature is in close agreement of the weather
287 station data, in terms of both magnitude and inter-annual variability. The annual mean wind
288 speed at MLW, a site near the shoreline, is comparable with the station data. At other more
289 exposed sites, the wind speed is much higher than observed at the WMO stations. The annual
290 mean relative humidity RH shows a larger spread among the eddy flux sites than among the
291 WMO stations partly because the measurement height at the eddy flux sites is not
292 standardized (Table 1). The upward trends in RH over time at DPK and XLS seem to be
293 related more to aging of the sensor than to a real inter-annual variability. We have not fully
294 investigated this aging problem, but it is possible to rectify it by doing a detailed regression
295 analysis against the station data.

296
297 Consistency of the energy flux variables can be evaluated with the energy balance closure.
298 Using observations made at a subset of the sites in the earlier years of the flux network,
299 Wang et al. (2014) reported a closure rate of 70 % to 110 % on the monthly basis, meaning
300 that the sum of the measured monthly sensible and the latent heat flux $H + \lambda E$ is 70 % to
301 110 % of the monthly available energy $R_n - G$, where R_n is net radiation and G is heat storage
302 in the water column. By selecting days without data gaps, we found that the daily energy
303 balance closure is in the range between 66 % and 78 % for all the lake sites and all the years.
304 Such closure rates are typical of eddy covariance observations (Tanny et al., 2008; Wilson et

305 al., 2002).

306

307 We have shown that the monthly latent heat flux at the lake sites MLW, BFG and DPK
308 during July 2010 to August 2012 follows the Priestley-Taylor (PT) model prediction with the
309 original PT constant α of 1.26 and that at the DS land site is in agreement with the PT model
310 if the constant is lowered to 1.0 (Lee et al., 2014). Figure 65 demonstrates that the same
311 relationships hold for all the sites and all the observational months, indicating the overall
312 stability of our measurement systems and the robustness of our gap-filling procedure. The
313 reader is reminded that the monthly latent heat flux in Figure 65 has been adjusted to force
314 energy closure following the method recommended by Barr et al. (1994), Blanken et al.
315 (1997) and Twine et al. (2000). (The half-hourly flux data in the data archive have not been
316 adjusted for energy balance.)

317

318 The Stefan-Boltzmann Law offers another way for checking data consistency. Because the
319 lake surface emits longwave radiation like a blackbody and because the annual mean air
320 temperature and the surface water temperature are nearly identical at this lake (Wang et al.,
321 2014), the change in the annual upward longwave radiation ΔL_{\uparrow} can be expressed as

$$322 \quad \Delta L_{\uparrow} = 4\sigma T_a^3 \Delta T_a$$

323 where T_a is annual mean air temperature, and Δ is the difference between the target year and
324 the year with the lowest air temperature observed at the site. All the five long-term lake sites
325 show good consistency between the longwave radiation and the air temperature observations
326 (Figure 76).

327

328 **6 Data availability**

329 All data can be open-accessed online for download and use at <https://yncenter.sites.yale.edu/>
330 and from Harvard Dataverse (<https://doi.org/10.7910/DVN/HEWCWM>, Zhang et al., 2020).

331

332 **7 Summary**

333 The dataset described here consists of microclimate variables (air temperature, air humidity,
334 wind speed, wind direction, water or soil temperature profile, and rainfall), four components
335 of the radiation balance, friction velocity, and sensible and latent heat fluxes observed at
336 seven lake sites and one land site. The period of coverage is from June 2010~~8~~ to December
337 2018. The observation interval is 30 min. Except for rainfall and wind direction, all other
338 variables have been gap-filled. Every data point is tagged with a data quality flag to help the
339 user determine how to best use the data.

340

341 **Author contribution**

342 XL, WX and MZ directed the field program, ZZ performed data gap-filling and prepared the
343 data for public release, CC, WW, CX, HC, JW, JZ, LJ, QL, WH, WZ, YL, YX, YW, YP, YH,
344 ZC and ZQ participated in field data collection, and ZZ, XL and MZ wrote the manuscript.

345

346 **Competing interests**

347 The authors declare no conflict of interest.

348

349 **Acknowledgments**

350 This work was supported by the National Key R&D Program of China (2019YFA0607202),
351 the National Natural Science Foundation of China (grant numbers 41575147, 41801093, and
352 41475141) and the Priority Academic Program Development of Jiangsu Higher Education
353 Institutions (grand number PAPD).

354

355

356

357

358 **Table 1.** A list of sites in the Lake Taihu Eddy Flux Network

Site ID	MLW	DPK	BFG	XLS	PTS	MLW2	DTH	DS
Lat (°N)	31.4197	31.2661	31.1685	30.9972	31.2323	31.3818	31.0611	31.0799
Long (°E)	120.2139	119.9312	120.3972	120.1344	120.1086	120.1608	120.4704	120.4346
Start date	Jun 2010	Aug 2011	Dec 2011	Nov 2012	Jun 2013	Feb 2018	Nov 2017	Apr 2011
Biology	Eutrophic	Super eutrophic	Submerged macrophyte	Transitional	Mesotrophic	Eutrophic	Aquaculture	Cropland/ Rural residence
Met height (m)	3.5	8.0	8.5	9.4	8.5	6.0	4.5	10.0
T _w / T _s depths (cm)	20, 50, 100, 150, sediment	20, 50, 100, 150, sediment	20, 50, 100, 150, sediment	20, 50, 100, 150, sediment	20, 50, 100, 150, sediment	20, 50, 100, 150, sediment	20, 50, sediment	5, 10, 20
Radiation height (m)	1.5	1.5	1.5	1.5	1.5	1.5	1.5	3.0
EC height (m)	3.5	8.5	8.5	9.4	8.5	6.0	4.5	20

359

360

361

362 **Table 2.** Percent of data coverage. The percentage represents the proportion of high-quality
363 original measurement.

Variable type	MLW	DPK	BFG	XLS	PTS	DTH	MLW2	DS
Micrometeorology	93.3	81.1	97.6	97.0	97.5	98.1	90.3	91.7
Radiation flux	85.5	90.8	96.9	97.4	98.6	98.2	98.2	82.7
Water/soil temperature	83.4	81.3	94.0	91.1	90.3	87.7	22.4	98.4
Eddy flux	73.3	61.8	82.7	79.1	80.6	85.7	85.5	82.8

364

365

366

367

368

369 **Table 3.** A list of data quality flags

Flag	Data quality description
0	Original data
1	Gap-filled with time interpolation
2	Gap-filled with spatial interpolation
3	Gap-filled with bulk relationship
4	NAN

370

371

373 **Table 4.** A list of data columns and variable definitions

Column	Description	Variable name	Unit
1	Year	Year	–
2	Month	Month	–
3	Day	Day	–
4	Hour	HH	–
5	Minute	MM	–
6	Day of Year	DOY	–
7	Air pressure	P	kPa
8	Quality flag of air pressure	P_flag	
9	Air temperature	Ta	°C
10	Quality flag of air temperature	Ta_flag	
11	Relative humidity	RH	%
12	Quality flag of Relative humidity	RH_flag	
13	Wind speed	WS	m s ⁻¹
14	Quality flag of wind speed	WS_flag	
15	Wind direction	WD	Degree
16	Quality flag of wind direction	WD_flag	
17	Rainfall	R	mm
18	Quality flag of rainfall	R_flag	
19	Upward shortwave radiation	UR	W m ⁻²
20	Quality flag of upward shortwave radiation	UR_flag	
21	Downward shortwave radiation	DR	W m ⁻²
22	Quality flag of downward shortwave radiation	DR_flag	
23	Upward longwave radiation	ULR	W m ⁻²
24	Quality flag of upward longwave radiation	ULR_flag	
25	Downward longwave radiation	DLR	W m ⁻²
26	Quality flag of downward longwave radiation	DLR_flag	
27	Water temperature at 0.2 m	T _{w_20}	°C

28	Quality flag of Water temperature at 0.2 m	T _{w_20_flag}	
29	Water temperature at 0.5 m	T _{w_50}	°C
30	Quality flag of Water temperature at 0.5 m	T _{w_50_flag}	
31	Water temperature at 1.0 m	T _{w_100}	°C
32	Quality flag of Water temperature at 1.0 m	T _{w_100_flag}	
33	Water temperature at 1.5 m	T _{w_150}	°C
34	Quality flag of water temperature at 1.5 m	T _{w_150_flag}	
35	Sediment temperature	T _{w_bot}	°C
36	Quality flag of sediment temperature	T _{w_bot_flag}	
37	Friction velocity	U*	m s ⁻¹
38	Quality flag of friction velocity	U*_flag	
39	Sensible heat flux	H	W m ⁻²
40	Quality flag of sensible heat flux	H_flag	
41	Latent heat flux	LE	W m ⁻²
42	Quality flag of latent heat flux	LE_flag	

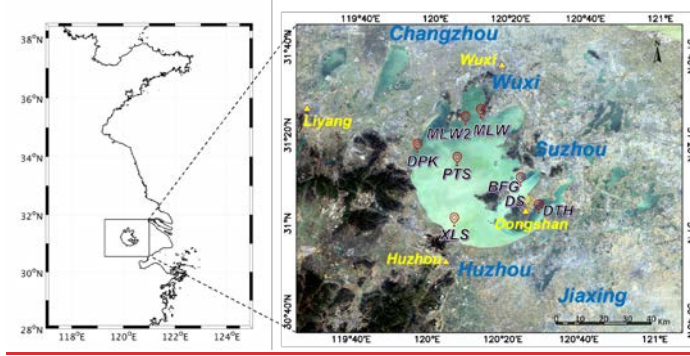
374 Notes: 1) Time marks end of a ~~half-hourly~~ observation in Beijing time (UTC+8:00); 2) At the DS site,
375 columns 27, 29, and 31 represent soil temperature at 5, 10, and 20 cm, respectively. column 33 represents
376 soil heat flux G (W m⁻²) measured at 5-cm depth, and column 34 represents quality flag of soil heat flux. Formatted: Superscript

377
378
379
380

381

382

383



384

385

386

387

388

389

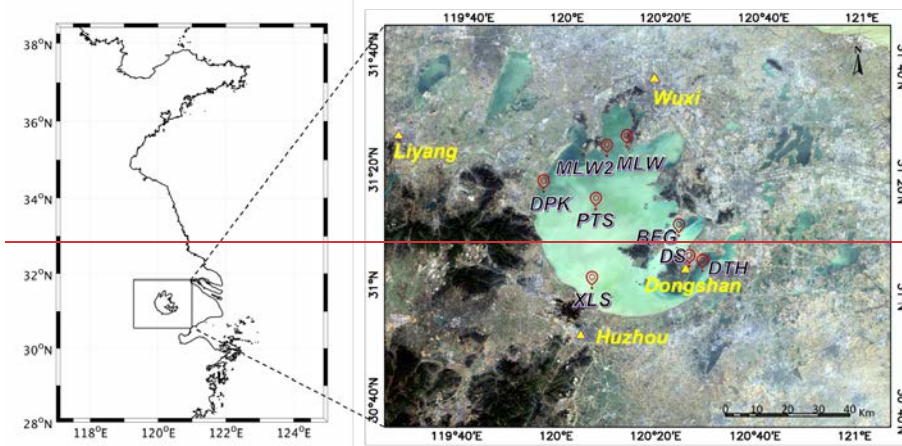
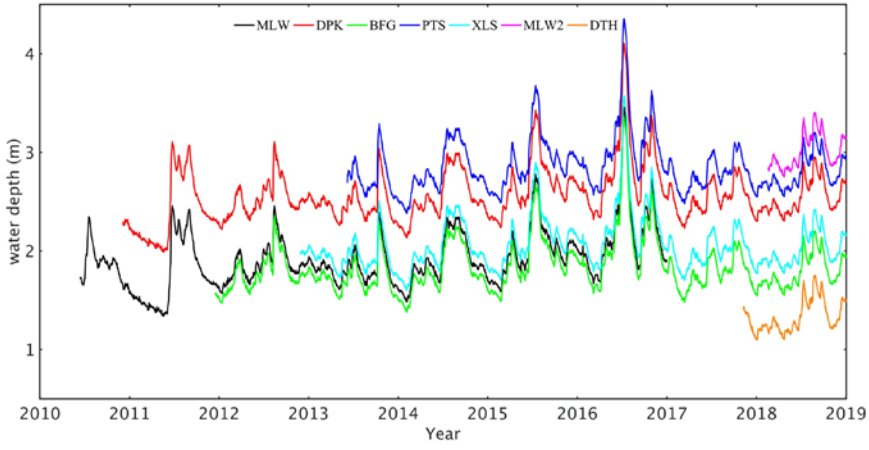


Figure 1. Map showing locations of Lake Taihu, eddy covariance sites (red bubbles) and WMO weather stations (yellow triangles). City names are shown in blue. DS is a land site, and MLW, MLW2, DPK, PTS, XLS, BFG and DTH are lake sites. The background is a natural color image from LANDSAT 8 without correction for atmospheric interference.

390



391

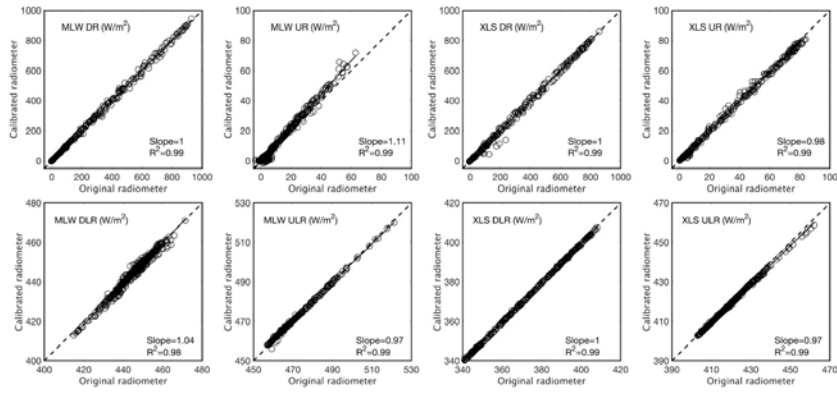
392 **Figure 2.** Water depth at the eddy covariance sites.

Formatted: Font : Bold

393

394

395
396
397



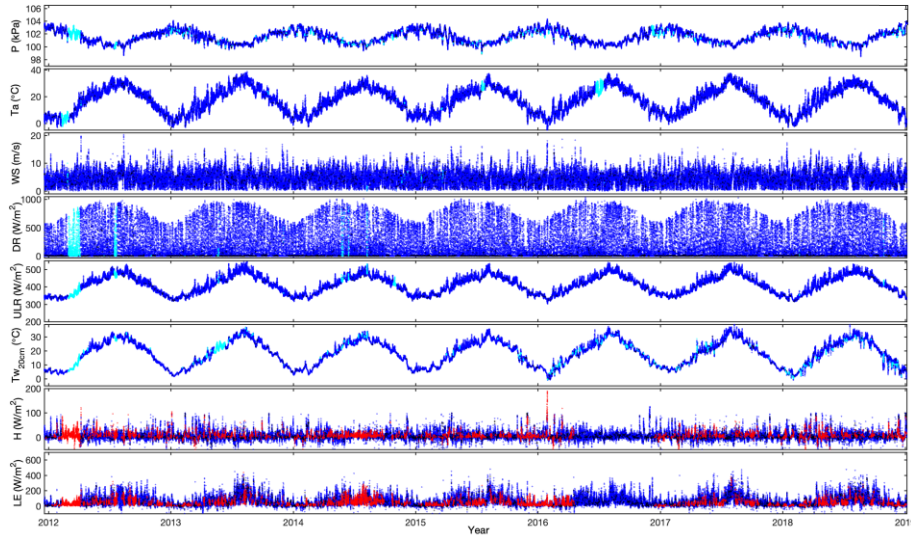
398

399 **Figure 32.** Comparison of four components of the radiation balance between the original
400 radiometer (horizontal axis) and a laboratory standard (vertical axis) at MLW and XLS. Refer
401 to Table 4 for variable definitions.

402
403

404

405



406

407 **Figure 43.** Complete gap-filled time series for selected variables observed at BFG. Blue,
408 black, cyan and red dots represent quality flag 0, 1, 2, and 3, respectively. Variable
409 definitions are given in Table 4

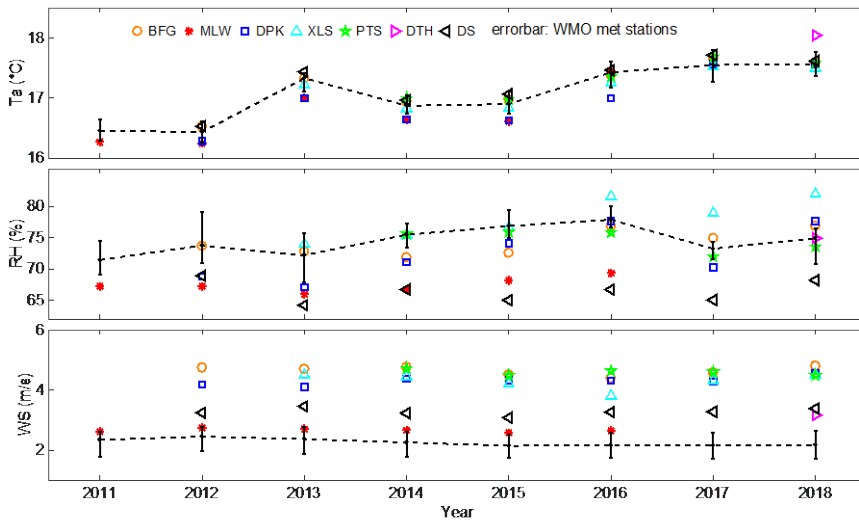
410

411

412

413

414



415

416

417

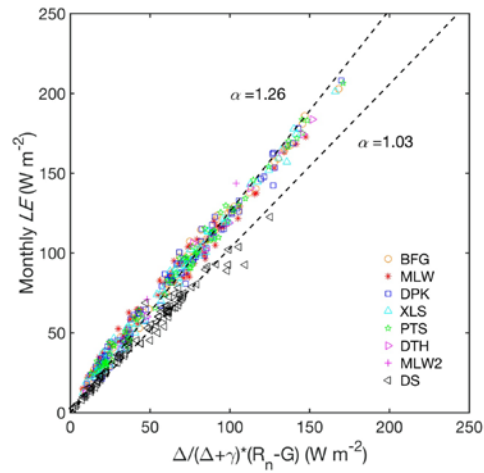
418

419

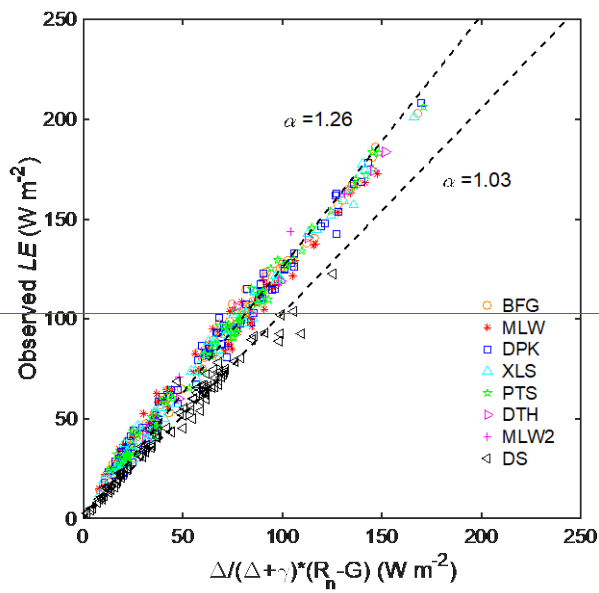
420

Figure 54. Annual mean air temperature (top), relative humidity (middle) and wind speed (bottom) observed at the eddy flux sites (symbols) and at the four WMO weather stations around the lake (line). Error bars represent the range of the annual means of the four WMO stations.

421



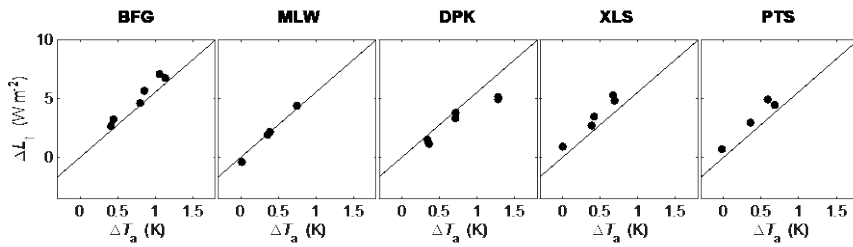
422



423

424 **Figure 65.** Comparison of observed monthly latent heat flux with Priestley-Taylor model
425 prediction using the original α coefficient of 1.26 and a modified coefficient of 1.03. Here
426 R_n is net radiation, G is heat storage in the water column, Δ is the slope of the saturation
427 vapor pressure curve, and γ is the psychrometric constant.

428



429
 430 **Figure 76.** The relationship between changes in observed annual mean upward longwave
 431 radiation flux and annual mean air temperature (dots). Solid lines represent the prediction of
 432 the Stefan-Boltzmann Law.
 433

434

435 **References**

- 436 Barr, A. G., King, K. M., Gillespie, T. J., Den Hartog, G. and Neumann, H. H.: A comparison of Bowen ratio
437 and eddy correlation sensible and latent heat flux measurements above deciduous forest, *Boundary-Layer*
438 *Meteorol.*, 71(1–2), 21–41, 1994.
- 439 Blanken, P. D., Black, T. A., Yang, P. C., Neumann, H. H., Nescic, Z., Staebler, R., Den Hartog, G., Novak, M.
440 D. and Lee, X.: Energy balance and canopy conductance of a boreal aspen forest: partitioning overstory and
441 understory components, *J. Geophys. Res. Atmos.*, 102(D24), 28915–28927, 1997.
- 442 Blanken, P. D., Spence, C., Hedstrom, N. and Lenters, J. D.: Evaporation from Lake Superior: 1. Physical
443 controls and processes, *J. Great Lakes Res.*, 37(4), 707–716, doi:10.1016/j.jglr.2011.08.009, 2011.
- 444 Charusombat, U., Fujisaki-Manome, A., Gronewold, A. D., Lofgren, B. M., Anderson, E. J., Blanken, P.,
445 Spence, C., Lenters, J. D., Xiao, C. and Fitzpatrick, L. E.: Evaluating and improving modeled turbulent heat
446 fluxes across the North American Great Lakes, *Hydrol. Earth Syst. Sci.*, 22(10), 2018.
- 447 Deng, B., Liu, S., Xiao, W., Wang, W., Jin, J. and Lee, X.: Evaluation of the CLM4 lake model at a large and
448 shallow freshwater lake, *J. Hydrometeorol.*, 14(2), 636–649, doi:10.1175/JHM-D-12-067.1, 2013.
- 449 Downing, J. A., Prairie, Y. T., Cole, J. J., Duarte, C. M., Tranvik, L. J., Striegl, R. G., McDowell, W. H.,
450 Kortelainen, P., Caraco, N. F., Melack, J. M. and Middelburg, J. J.: The global abundance and size distribution
451 of lakes, ponds, and impoundments, *Limnol. Oceanogr.*, 51(5), 2388–2397, doi:10.4319/lo.2006.51.5.2388,
452 2006.
- 453 Du, Q., Liu, H., Xu, L., Liu, Y. and Wang, L.: The monsoon effect on energy and carbon exchange processes
454 over a highland lake in the southwest of China, *Atmos. Chem. Phys.*, 18(20), 15087–15104, 2018.
- 455 Franz, D., Mammarella, I., Boike, J., Kirillin, G., Vesala, T., Bornemann, N., Larmanou, E., Langer, M. and
456 Sachs, T.: Lake-atmosphere heat flux dynamics of a thermokarst lake in arctic Siberia, *J. Geophys. Res. Atmos.*,
457 123(10), 5222–5239, 2018.
- 458 Franz, D., Mammarella, I., Boike, J., Kirillin, G., Vesala, T., Bornemann, N., Larmanou, E., Langer, M. and
459 Sachs, T.: Lake-atmosphere heat flux dynamics of a thermokarst lake in arctic Siberia, *J. Geophys. Res. Atmos.*,
460 123(10), 5222–5239, 2018.
- 461 Hamdani, I., Assouline, S., Tanny, J., Lensky, I. M., Gertman, I., Mor, Z. and Lensky, N. G.: Seasonal and
462 diurnal evaporation from a deep hypersaline lake: the Dead Sea as a case study, *J. Hydrol.*, 562, 155–167, 2018.
- 463 Hu, C., Wang, Y., Wang, W., Liu, S., Piao, M., Xiao, W. and Lee, X.: Trends in evaporation of a large
464 subtropical lake, *Theor. Appl. Climatol.*, 129(1–2), 159–170, doi:10.1007/s00704-016-1768-z, 2017.
- 465 Lee, X., Massman, W. and Law, B.: *Handbook of micrometeorology: a guide for surface flux measurement and*
466 *analysis*, Springer Science & Business Media., 2004.

467 Lee, X., Liu, S., Xiao, W., Wang, W., Gao, Z., Cao, C., Hu, C., Hu, Z., Shen, S., Wang, Y., Wen, X., Xiao, Q.,
468 Xu, J., Yang, J. and Zhang, M.: The taihu eddy flux network: An observational program on energy, water, and
469 greenhouse gas fluxes of a large freshwater lake, *Bull. Am. Meteorol. Soc.*, 95(10), 1583–1594,
470 doi:10.1175/BAMS-D-13-00136.1, 2014.

471 Li, Z., Lyu, S., Ao, Y., Wen, L., Zhao, L. and Wang, S.: Long-term energy flux and radiation balance
472 observations over Lake Ngoring, Tibetan Plateau, *Atmos. Res.*, 155, 13–25, 2015.

473 Nordbo, A., Launiainen, S., Mammarella, I., Leppäranta, M., Huotari, J., Ojala, A. and Vesala, T.: Long-term
474 energy flux measurements and energy balance over a small boreal lake using eddy covariance technique, *J.*
475 *Geophys. Res. Atmos.*, 116(D2), 2011.

476 Subin, Z. M., Riley, W. J. and Mironov, D.: An improved lake model for climate simulations: Model structure,
477 evaluation, and sensitivity analyses in CESM1, *J. Adv. Model. Earth Syst.*, 4(2), 1–27,
478 doi:10.1029/2011MS000072, 2012.

479 Tanny, J., Cohen, S., Assouline, S., Lange, F., Grava, A., Berger, D., Teltch, B. and Parlange, M. B.:
480 Evaporation from a small water reservoir: Direct measurements and estimates, *J. Hydrol.*, 351(1–2), 218–229,
481 2008.

482 Twine, T. E., Kustas, W. P., Norman, J. M., Cook, D. R., Houser, Pr., Meyers, T. P., Prueger, J. H., Starks, P. J.
483 and Wesely, M. L.: Correcting eddy-covariance flux underestimates over a grassland, *Agric. For. Meteorol.*,
484 103(3), 279–300, 2000.

485 Verpoorter, C., Kutser, T., Seekell, D. A. and Tranvik, L. J.: A global inventory of lakes based on
486 high-resolution satellite imagery, *Geophys. Res. Lett.*, 41(18), 6396–6402, doi:10.1002/2014GL060641, 2014.

487 Vesala, T., Huotari, J., Rannik, Ü., Suni, T., Smolander, S., Sogachev, A., Launiainen, S. and Ojala, A.: Eddy
488 covariance measurements of carbon exchange and latent and sensible heat fluxes over a boreal lake for a full
489 open-water period, *J. Geophys. Res. Atmos.*, 111(11), 1–12, doi:10.1029/2005JD006365, 2006.

490 Wang, B., Ma, Y., Wang, Y., Su, Z. and Ma, W.: Significant differences exist in lake-atmosphere interactions
491 and the evaporation rates of high-elevation small and large lakes, *J. Hydrol.*, 573, 220–234, 2019.

492 Wang, W., Xiao, W., Cao, C., Gao, Z., Hu, Z., Liu, S., Shen, S., Wang, L., Xiao, Q., Xu, J., Yang, D. and Lee,
493 X.: Temporal and spatial variations in radiation and energy balance across a large freshwater lake in China, *J.*
494 *Hydrol.*, 511, 811–824, doi:10.1016/j.jhydrol.2014.02.012, 2014.

495 Wang, Y., Gao, Y., Qin, H., Huang, J., Liu, C., Hu, C., Wang, W., Liu, S. and Lee, X.: Spatiotemporal
496 Characteristics of Lake Breezes over Lake Taihu, China, *J. Appl. Meteorol. Climatol.*, 56(7), 2053–2065, 2017.

497 Webb, E. K., Pearman, G. I. and Leuning, R.: Correction of flux measurements for density effects due to heat
498 and water vapour transfer, *Q. J. R. Meteorol. Soc.*, 106(447), 85–100, 1980.

499 Wilson, K., Goldstein, A., Falge, E., Aubinet, M., Baldocchi, D., Berbigier, P., Bernhofer, C., Ceulemans, R.,

500 Dolman, H. and Field, C.: Energy balance closure at FLUXNET sites, *Agric. For. Meteorol.*, 113(1–4), 223–243,
501 2002.

502 Xiao, K., Griffis, T. J., Baker, J. M., Bolstad, P. V., Erickson, M. D., Lee, X., Wood, J. D., Hu, C. and Nieber, J.
503 L.: Evaporation from a temperate closed-basin lake and its impact on present, past, and future water level, *J.*
504 *Hydrol.*, 561, 59–75, 2018.

505 Xiao, W., Liu, S., Wang, W., Yang, D., Xu, J., Cao, C., Li, H. and Lee, X.: Transfer Coefficients of Momentum,
506 Heat and Water Vapour in the Atmospheric Surface Layer of a Large Freshwater Lake, *Boundary-Layer*
507 *Meteorol.*, 148(3), 479–494, doi:10.1007/s10546-013-9827-9, 2013.

508 Xiao, W., Liu, S., Li, H., Xiao, Q., Wang, W., Hu, Z., Hu, C., Gao, Y., Shen, J., Zhao, X., Zhang, M. and Lee,
509 X.: A flux-gradient system for simultaneous measurement of the CH₄, CO₂, and H₂O fluxes at a lake-air
510 interface, *Environ. Sci. Technol.*, 48(24), 14490–14498, doi:10.1021/es5033713, 2014.

511 Xu, J., Lee, X., Xiao, W., Cao, C., Liu, S., Wen, X., Xu, J., Zhang, Z. and Zhao, J.: Interpreting the ¹³C/¹²C ratio
512 of carbon dioxide in an urban airshed in the Yangtze River Delta, China, *Atmos. Chem. Phys.*, 17(5),
513 doi:10.5194/acp-17-3385-2017, 2017.

514 Yusup, Y. and Liu, H.: Effects of Atmospheric Surface Layer Stability on Turbulent Fluxes of Heat and Water
515 Vapor across the Water–Atmosphere Interface, *J. Hydrometeorol.*, 17(11), 2835–2851, 2016.

516 Zhang, M., Xiao, Q., Zhang, Z., Gao, Y., Zhao, J., Pu, Y., Wang, W., Xiao, W., Liu, S. and Lee, X.: Methane
517 flux dynamics in a submerged aquatic vegetation zone in a subtropical lake, *Sci. Total Environ.*, 672,
518 doi:10.1016/j.scitotenv.2019.03.466, 2019a.

519 Zhang, X., Huang, J., Li, G., Wang, Y., Liu, C., Zhao, K., Tao, X., Hu, X.-M. and Lee, X.: Improving
520 Lake-Breeze Simulation with WRF Nested LES and Lake Model over a Large Shallow Lake, *J. Appl. Meteorol.*
521 *Climatol.*, 58(8), 1689–1708, 2019b.

522 Zhang, Z., Zhang, M., Cao, C., Wang, W., Xiao, W., Xie, C., Chu, H., Wang, J., Zhao, J., Jia, L., Liu, Q.,
523 Huang, W., Zhang, W., Lu, Y., Xie, Y., Wang, Y., Pu, Y., Hu, Y., Chen, Z., Qin, Z. and Lee, X.: A dataset of
524 microclimate and radiation and energy fluxes from the Lake Taihu Eddy Flux Network, Harvard Dataverse,
525 <https://doi.org/10.7910/DVN/HEWCWM>, 2020

526 Zhao, X. and Liu, Y.: Variability of surface heat fluxes and its driving forces at different time scales over a large
527 ephemeral lake in China, *J. Geophys. Res. Atmos.*, 123(10), 4939–4957, 2018.

528